




## Control Algorithm for Renewable Energy Standalone System with Power Quality and Demand Management

Lingappa Jaklair<sup>1</sup>, Guduri Yesuratnam<sup>2</sup>, Pannala Mallikarjuna Sarma<sup>3</sup>

1,2 -Electrical Engineering Department, University College of Engineering, Osmania University, Hyderabad, India.

E-mail: lingappa.ou@gmail.com (Corresponding author) , ratnamgy2003@gmail.com

3-Electrical Engineering Department, Vasavi College of Engineering, Hyderabad, India.

Email: pmsarma2010@gmail.com

### ABSTRACT:

This paper deals with the problems related to power stability issues in the isolated wind-solar based renewable energy system. The stability issues in such system are produced mainly due to unbalanced loading, distortion of load current and intermittent nature of renewable energy sources. To overcome these problems, A voltage source converter (VSC) is used in proposed literature. The VSC is driven using a time domain-based signal decomposition algorithm consisting a 3-phase dual reduced order generalized integrators frequency Locked loop (DROGI-FLL). The 3 phase DROGI FLL has the inherent abilities of noise rejection and error tracking, which improves the system stability and maintains the voltage and frequency of the system constant under transient conditions. The transient conditions are simulated by varying the loading condition, solar irradiance and wind speed in the system. Apart from stability issues this system also deals with the issues related to reactive composition, natural current compensation and operation of SPV system at maximum power point (MPP). A perturb and observe (P&O) maximum power point tracking (MPPT) is employed for the working of solar photovoltaic systems (SPV) system at MPP and to maximize the utilization of renewable energy. The neutral current compensation is achieved by using a star-double delta transformer. This entire system is developed and tested in the MATLAB/SIMULINK environment.

**KEYWORDS:** Voltage Source Converter, Power Quality, DROGI-FLL, Time Domain-Based Signal Decomposition, Wind-Solar Energy System, Load Balance, Demand Response.

### 1. INTRODUCTION

Problems related to environment such as global warming; pollution has become more severe in recent years. The use of fossil fuel to generate electricity is one of the main reasons for the environmental problems. Still, some parts in the world does not have access to the electricity through conventional system [1]. According to the international energy agency's world energy access report, 2017 about 1.1 billion people are still living without access to electricity. So, to tackle this problem without breaking the demand-supply chain the use of isolated renewable energy sources has increased rapidly in past few years. Renewable energy systems are environment friendly sources of energy [2]. Solar, wind, tidal, hydro, bio-mass are some of the various type of renewable energy sources [3]. The adequate amount of wind energy is available in hilly area and near to sea shore regions. Therefore, it is the most popular choice rather than other non-conventional sources of energy for remote locations [4]. The self-excited induction generator (SEIG) is widely used to harvest wind energy because of its enormous advantages. The SEIG has natural protection against short

©The Author(s) 2024

Paper type: Research paper

<https://doi.org/10.30486/mjee.2024.2006726.1363>

Received: 9 October 2023; revised: 10 November 2023; accepted: 28 December 2023; published: 1 March 2024

How to cite this paper: L. Jaklair, G. Yesuratnam, and P. Mallikarjuna Sarma, "Control Algorithm for Renewable Energy Standalone System with Power Quality and Demand Management", *Majlesi Journal of Electrical Engineering*, Vol. 18, No. 1, pp. 311-322, 2024.

circuit and over current through its terminals, robust and solid rotor, its rotor construction is suitable for high speeds and it also accepts constant and variable loads, starts either loaded or without loaded [5]. But the voltage and frequency of the generated output has to be maintained within permissible limit under varying loading condition when SEIG is operated in isolated mode [6]. For this, many voltage and frequency controllers have been developed for SEIG. The earlier stage controllers are phase controlled bridge [7]. Uncontrolled rectifier and DC chopper [8]. Neither real power nor reactive power is supplied by these controllers into the system. Hence, required large capacitor bank for the excitation of the SEIG. And apart from that, these controllers have poor power factor and inject voltage and current harmonics in the system. To overcome above mentioned problems, a three-phase current controlled VSC is presented in [9-10]. The required voltage to drive the VSC is build up through battery energy storage system (BESS) along with SPV array. The BESS is used to mitigate the negative effect of dynamic disturbance which enhance the stability of the power system, but some time it creates unexpected degradation in power quality [11]. To overcome those problem via implementing the SPV which has advantages like ease of availability, nature friendly in manner and operating cost is much less. However, it is intermittent in nature like non-sunny days. So, alone SPV does not fulfill the demand of the load every time, which also reduces the reliability and performance of the system [12-13]. The disadvantage of BESS and SPV is eliminated by using combined SPV-BESS. To extract maximum power from the solar, MPPT technique is employed in SPV system. There are various MPPT techniques are represented in existing literatures. However, perturb and observe MPPT technique is widely used due to ease of implementation, simplicity and good performance [14]. The required gate pulse to drive the VSC is provided by pulse width modulation (PWM) control. The PWM compares two signals i.e., carrier signal and modulation signal. The high frequency triangular wave used as a carrier signal. The modulation signal is generated using various synchronizing techniques. Various synchronizing techniques are already present in existing literatures, but phase-locked-loop (PLL) are widely employed in the power-electronics and power system application. Several advanced PLL have been proposed having in loop filtering stage to improve the detection speed but the further improvement in PLL's dynamic performance without compromising their disturbance rejection capability and stability. To overcome this problem in [15] a novel type-1 FLL is proposed, having several advantages like better performance in dynamic condition and higher stability margins.

This paper introduces the implementation of DROGI-FLL to improve the stability of the voltage and frequency in standalone hybrid solar - wind based system. Moreover, balancing of the load at generator terminal, compensation of the load harmonics and compensation of the fourth wire current in various load conditions have been reduced. The negative sequence component is also extract by DROGI-FLL. This several features of the mentioned algorithm shows capabilities with solar-wind based hybrid generating system where the wind of wind turbine and irradiation of SPV is intermittent in nature.

## 2. SYSTEM CONFIGURATION

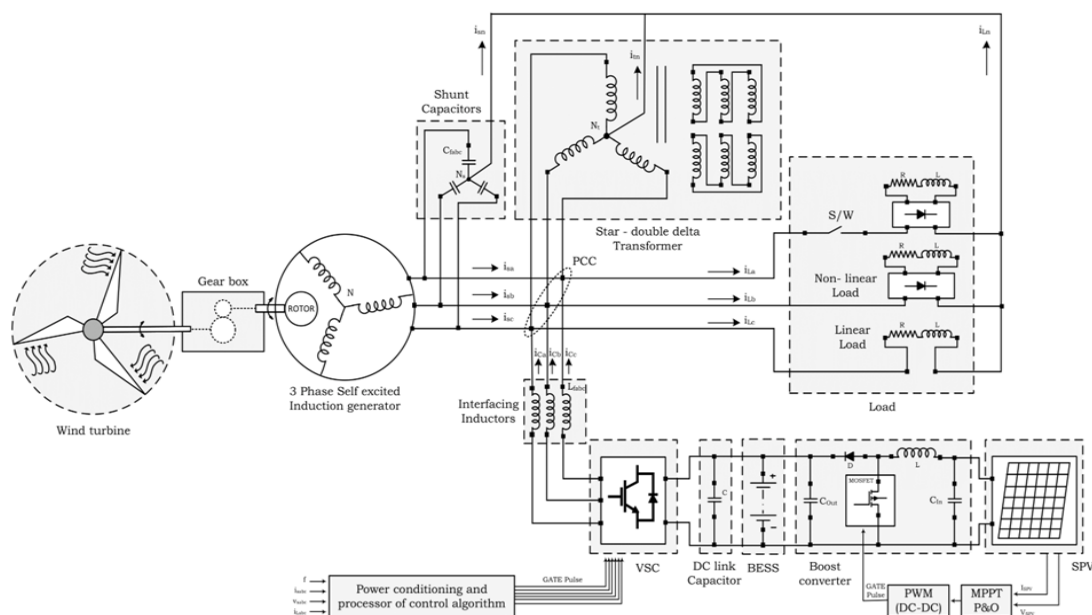


Fig. 1. Schematic diagram of the system to be study.

In Fig. 1 a three-blade wind generator coupled with three phase SEIG is shown. A star connected capacitor bank is connected across generator terminal to help building up no load voltage. A mixed load is connected with generator, where phase “a” and phase “c” are loaded with non-linear RL load and phase “b” is loaded with linear RL type load.

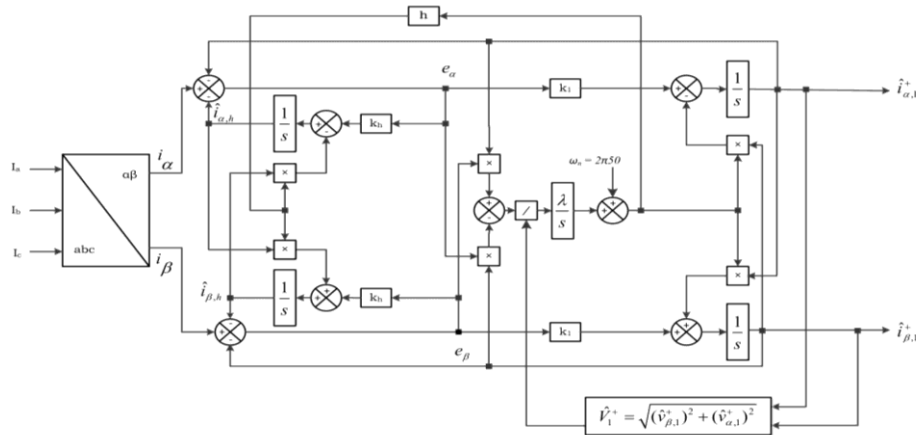


Fig.2. Block diagram of FLL based DROGI controller

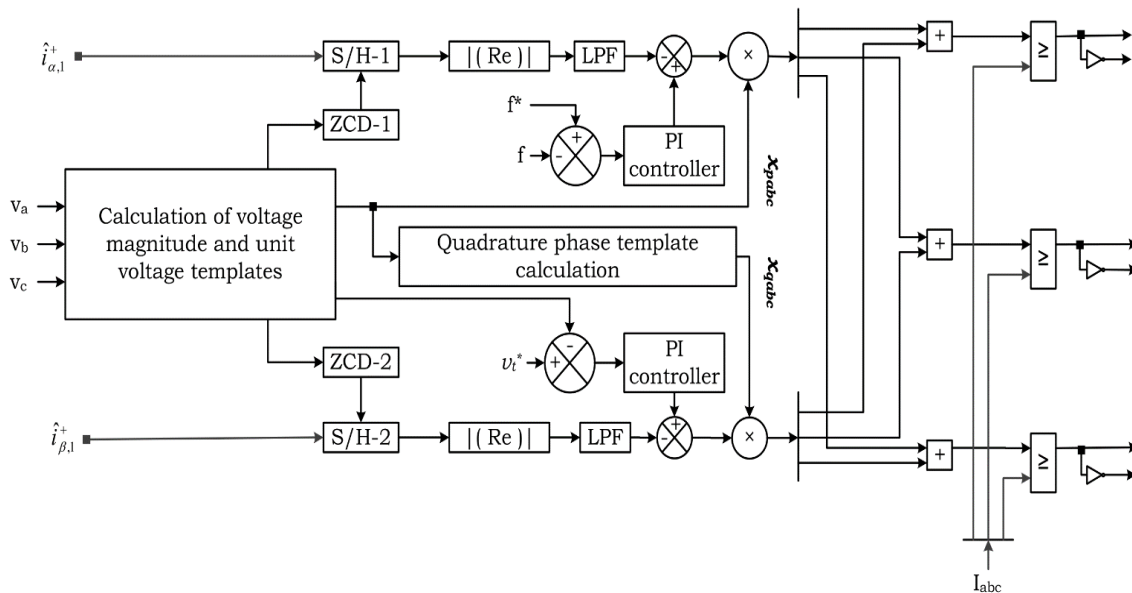


Fig.2. Control block diagram with Unit- voltage template

A VSC is connected at point of common coupling (PCC) with the help of interfacing inductors. A BESS and SPV array with DC-DC boost converter are connected across the DC link. One star - double delta transformer is also connected at PCC for neutral current compensation. The purpose of VSC is to compensate harmonic and reactive power of the load current which contains 3- legs (6 – Insulated gate bipolar transistors), three phase interfacing inductors, DC link capacitor. The BESS and SPV system are used to maintain the required voltage across DC-link capacitor. MPPT is used for extracting maximum power from SPV array.

### 3. ALGORITHM DETAILS

A time domain signals decomposition algorithm based DROGI-FLL is employed in this paper. It is a non-linear feedback control system which is tuned for two concerned frequency components. In addition to that, P&O MPPT is also used to operate SPV system at MPP. This technique is simple and effective. The boost converter is also used to

boost the output voltage of SPV. The intermittent nature of renewable energy sources is also simulated in this paper by varying the input conditions of the wind turbine and SPV system.

### 3.1. DROGI Algorithm

The current controller used in the power system has the generalized integrator as its building block. ROGI is used in this paper because it fulfills the basic requirements of hybrid renewable power system such as power quality, grid synchronization, and successful handling of severe voltage unbalanced conditions. The active power injection strategies used in ROGI requires very low computational effort and does not require any dedicated synchronization algorithm [16].

The ROGI is written as following in Laplace domain,

$$G_{ROGI}(s) = \frac{1}{s - j\omega C} \quad (1)$$

Various combinations can be designed using multiple ROGIs according to the application. Here we have taken parallel combination of two ROGIs which is shown in Fig. (2). One of which is centered at fundamental positive order frequency and another is centered at negative order disturbance frequency. And to make the centre frequency adaptive to frequency changes, FLL is used. Here, the input signal of FLL consists of two components, first is the fundamental components and second is harmonics components which is to be eliminated.

$$\begin{pmatrix} i_a \\ i_b \\ i_c \end{pmatrix} = \begin{pmatrix} I_1^+ \cos \theta_1^+ \\ I_1^+ \cos(\theta_1^+ - 2\pi/3) \\ I_1^+ \cos(\theta_1^+ + 2\pi/3) \end{pmatrix} + \begin{pmatrix} I_h \cos \theta_h \\ I_h \cos(\theta_h - 2\pi/3) \\ I_h \cos(\theta_h + 2\pi/3) \end{pmatrix} \quad (2)$$

Where,  $I_1^+$  denotes the amplitude and  $\theta_1^+$  denotes phase angle of fundamental frequency positive sequence (FFPS) and  $I_h$  and  $\theta_h$  denotes amplitude and phase angle of h-order frequency component respectively. Here the h is taken as “-1”. So, the h-order component stands for fundamental frequency negative sequence component. Converting above equation in  $\alpha\beta$  frame, which can be written as

$$\begin{pmatrix} i_\alpha \\ i_\beta \end{pmatrix} = \begin{pmatrix} I_1^+ \cos \theta_1^+ \\ I_1^+ \sin \theta_1^+ \end{pmatrix} + \begin{pmatrix} I_h \cos \theta_h \\ I_h \sin \theta_h \end{pmatrix} \quad (3)$$

From equation (3), it can be concluded that the signals extracted by DROGI-FLL should be in the given form.

$$\begin{pmatrix} \hat{i}_{\alpha,1}^+ \\ \hat{i}_{\beta,1}^+ \end{pmatrix} = \begin{pmatrix} \hat{I}_1^+ \cos(\hat{\theta}_1) \\ \hat{I}_1^+ \sin(\hat{\theta}_1) \end{pmatrix} \begin{pmatrix} \hat{i}_{\alpha,h} \\ \hat{i}_{\beta,h} \end{pmatrix} = \begin{pmatrix} \hat{I}_h \cos(\hat{\theta}_h) \\ \hat{I}_h \sin(\hat{\theta}_h) \end{pmatrix} \quad (4)$$

The actual parameters  $I_1^+$ ,  $\theta_1^+$ ,  $I_h$ ,  $\theta_h$  and their estimations are defined as a sum of nominal value (indicating by subscript) and a small perturbation (indicated by  $\Delta$ ), as follows

$$\begin{aligned} I_1^+ &= I_{n,1}^+ + \Delta I_1^+, & \hat{I}_1^+ &= I_{n,1}^+ + \Delta \hat{I}_1^+ \\ \theta_1^+ &= \theta_{n,1}^+ + \Delta \theta_1^+, & \hat{\theta}_1^+ &= \theta_{n,1}^+ + \Delta \hat{\theta}_1^+ \\ I_h &= I_{n,h} + \Delta I_h, & \hat{I}_h &= I_{n,h} + \Delta \hat{I}_h \\ \theta_h &= \theta_{n,h} + \Delta \theta_h, & \hat{\theta}_h &= \theta_{n,h} + \Delta \hat{\theta}_h \end{aligned} \quad (5)$$

Where,  $\Theta_{n,1}^+ = \omega_n t$  and  $\Theta_{n,h} = h\omega_n t + \delta_h$ . The fundamental angular frequency of grid and its estimation are also defined as

$$\begin{aligned} \omega &= \omega_n + \Delta\omega \\ \hat{\omega} &= \omega_n + \Delta\hat{\omega} \end{aligned} \tag{6}$$

Where,  $\omega_n = 2\pi 50$  rad/s

### 3.2. Unit Templates and Signal Conditioning

For the generation of Reference current Signal, the Unit - Voltage Template is required. This unit voltage Templates are calculated from amplitude of generator terminal voltage (Vt). From this Vt, active and Reactive Unit voltage Templates are calculated [17]. The actual frequency & Ref freq. is compared and error signal generated is given to The PI Controller. The active Current extracted from DROGI Controller & o/p Current of Solar PV system is then added to the Current produced by PI Controller. Similarly, the Terminal Voltage & Ref-voltage is compared and o/p signal is given to another PI controller, whose o/p is then subtracted from reactive component produced by D-ROGI controller. With the help of active, reactive ref-currents and unit templates signal, reference current signal is produced. The actual (source) & ref. Current signals are compared and the error is processed by PWM for generation of gate signals.

### 3.3. MPPT Algorithm

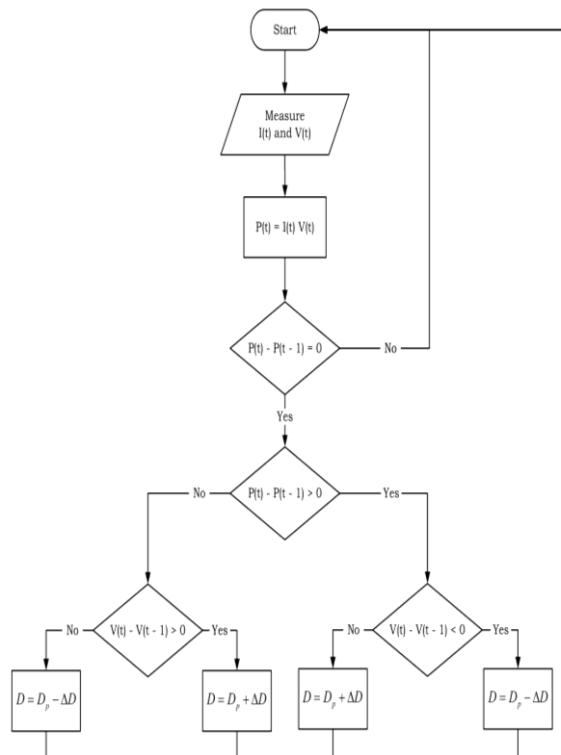


Fig.3. Flowchart of perturb and observe technique.

MPPT is to achieve maximum power output in PV array according to irradiance, temperature and load current variation. Different MPPT techniques are described in literatures but their suitability mainly depends on factors like the dynamics of irradiance, design simplicity, convergence speed, cost and hardware implementation [18]. From all available techniques the P&O method is widely used because of its simplicity, ease of implementation and better performance. In the P&O algorithm, the power is obtained from output i.e., voltage and current of the PV array. Now, the power is checked by varying voltage.

There are four cases,

Case (a) : If power of array increases and voltage of array also increases then the duty cycle is to be reduced.

- Case (b) : If power of array increases and voltage of array decreases then the duty cycle is to be increased.  
 Case (c) : If power of array decreases and voltage of array increases then the duty cycle is to be reduced.  
 Case (d) : If power of array decreases and voltage of array also decreases then the duty cycle is to be increased.

### 3.4 Boost Converter

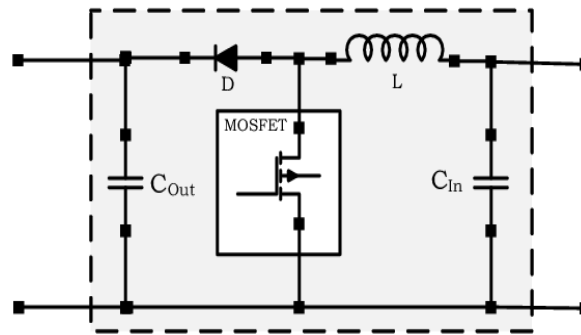


Fig. 5. Circuit diagram of DC-DC boost converter.

A DC-DC boost converter is used to achieve MPP with the advantages of less components to reduce implementation cost and high reliability. It consists of a power MOSFET used as a switching transistor. The gate pulses of the MOSFET are provided from PWM which is controlled by MPPT output.

## 4. SIMULATION RESULT

A Simulink model consisting a wind-solar based renewable energy system is developed as shown in Fig. (1). The entire simulation is simulated at 10  $\mu$ sec periodic sampling time ( $T_s$ ). The active and reactive component of load current is estimated using DROGI-FLL. The parameters at which system is simulated are given in appendix. The system is tested for the stability in the transient conditions such as change in irradiance of SPV system, unbalanced loading and change in wind speed of wind generator. There are three single phase loads connected to individual phases and are of R-L type. Two of those three phase loads (loads connected on phase A and phase C) consist a diode bridge making them non-linear type of loads. The measurement of the voltage is done on phase to ground basis. The result of this simulation is given in case-by-case manner.

**Case (a):** The response of the system under change in irradiation (Irr) of SPV system is plotted in Fig. (6). The irradiance of the SPV system is changed from 800W/m<sup>2</sup> to 1000W/m<sup>2</sup> at  $t=3.00$  sec, keeping the wind speed and the loads constant. As the irradiance increases, the increase in the current of SPV system ( $I_{spv}$ ) can also be seen increasing in Fig. (6). This increase in current also lets SPV system produce more power output. The P&O MPPT algorithm employed along with boost converter varies the duty cycle of the gate pulses given to MOSFET switch of boost converter. During this time the system voltage could be seen constant and following the reference line (shown by dotted line). And similarly, the frequency of the system also remains close to reference. This ability of system to maintain the voltage and frequency constant makes it perfectly stable and can handle such transients.

**Case(b):** The change in system performance under unbalanced loading condition is been studied in this case. The wind speed and the irradiation are kept constant while simulating this dynamic condition. The load on phase A is thrown off at  $t = 3.5$  sec for simulating unbalanced loading condition. As seen in the Fig. (7), the load current of phase A becomes zero at  $t = 3.5$  sec. But even when load is unbalanced the system voltage and frequency can be seen unaffected as the compensator work efficiently and uses the BESS as dump load for maintaining generator current ( $I_{abc}$ ) balanced. This feature of this system makes it much stable in such transient conditions. The Compensator current after  $t = 3.5$  sec can be seen changed and become more sinusoidal which will be then filtered by interfacing inductors. The neutral point at load side also changes as the load on system gets unbalanced, but the compensating transformer works satisfactory and compensates the neutral current, which makes the neutral current at generator almost zero.

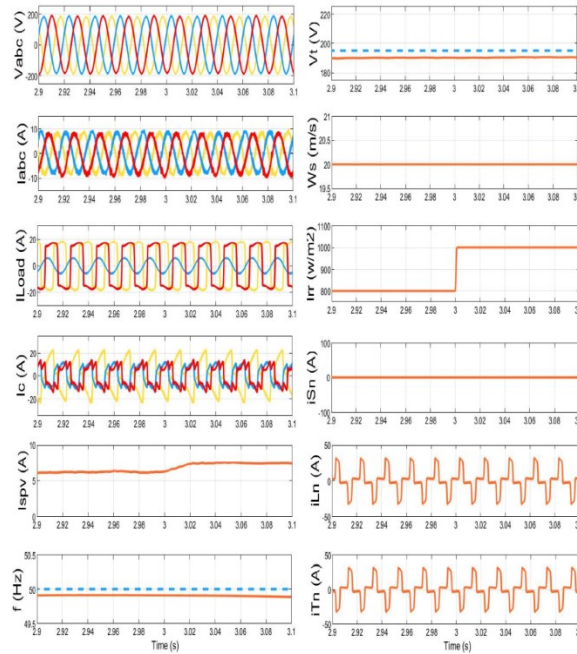


Fig. 4. (a)  $V_{abc}$  = Three phase generator voltage, (b)  $I_{abc}$  = Three phase generator current, (c)  $I_{Load}$  = Three phase load current, (d)  $I_c$  = Compensator current, (e)  $I_{spv}$  = Solar photo-voltaic current, (f)  $f$  = frequency of system, (g)  $V_t$  = Generator terminal voltage, (h)  $W_s$  = Wind turbine speed, (i)  $I_{rr}$  = Irradiation of SPV, (j)  $i_{Sn}$  = Nutral current of Generator, (k)  $i_{Ln}$  = Nutral current of Load, (l)  $i_{Tn}$  = Nutral current of transformer

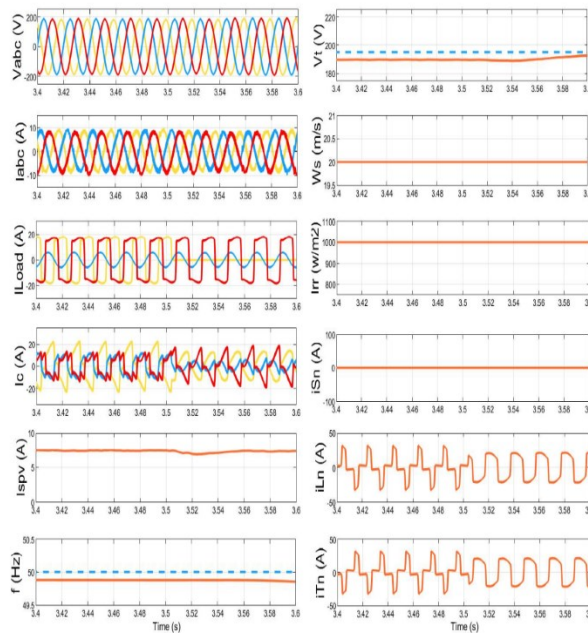


Fig.5. (a)  $V_{abc}$  = Three phase generator voltage, (b)  $I_{abc}$  = Three phase generator current, (c)  $I_{Load}$  = Three phase load current, (d)  $I_c$  = Compensator current, (e)  $I_{spv}$  = Solar photo-voltaic current, (f)  $f$  = frequency of system, (g)  $V_t$  = Generator terminal voltage, (h)  $W_s$  = Wind turbine speed, (i)  $I_{rr}$  = Irradiation of SPV, (j)  $i_{Sn}$  = Nutral current of Generator, (k)  $i_{Ln}$  = Nutral current of Load, (l)  $i_{Tn}$  = Nutral current of transformer

**Case(c):** The intermittent nature of wind energy could break the stability of the system. So, in this case, the variation in wind speed is simulated by changing the speed of the wind turbine. At  $t=4.2$  sec, the wind speed ( $W_s$ ) is increased from 20 m/s to 20.5 m/s. The change in wind speed causes the change in speed of wind turbine and hence changing speed of the rotor of the SEIG. As there is no such mechanical governor system to control such variation, the compensator has to work for it. The compensator provides such a governing effect, by which the effect of change in wind speed is almost nullified and it can be seen in Fig. (8), as the plot of frequency and the terminal voltage shows no major deviation. This increase in the wind speed, gives rise in the power of the system developed by the wind generator. From the response seen in the Fig. (8), there is significant effect of change in wind speed could be observed. And as seen in the Fig. (8), the solar irradiation is kept 1000 w/m<sup>2</sup> and the load on the system is kept constant.

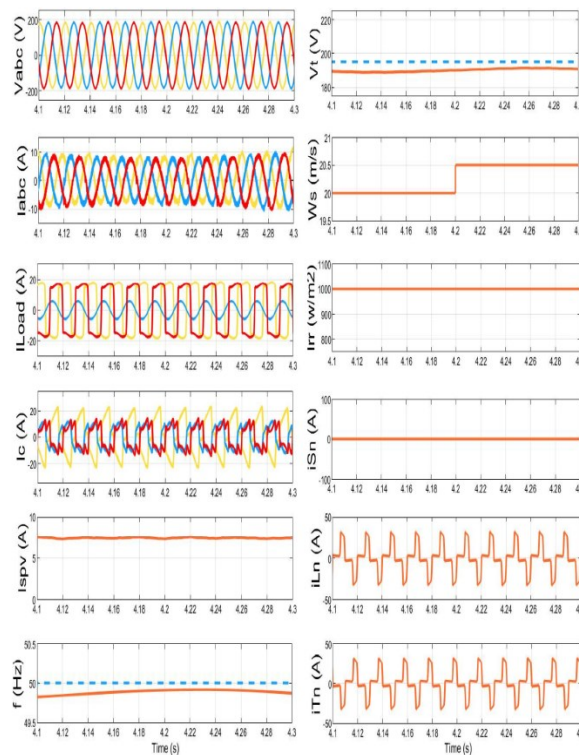


Fig. 6. (a)  $V_{abc}$  = Three phase generator voltage, (b)  $I_{abc}$  = Three phase generator current, (c)  $I_{Load}$  = Three phase load current, (d)  $I_c$  = Compensator current, (e)  $I_{spv}$  = Solar photo-voltaic current, (f)  $f$  = frequency of system, (g)  $V_t$  = Generator terminal voltage, (h)  $W_s$  = Wind turbine speed, (i)  $I_{rr}$  = Irradiation of SPV, (j)  $i_{Sn}$  = Neutral current of Generator, (k)  $i_{Ln}$  = Neutral current of Load, (l)  $i_{Tn}$  = Neutral current of transformer

**Case(d):** The active and reactive power of the various components of the system is plotted in Fig. (9). The wind energy generation system requires some time to get energised and start working, as SEIG is used as generator. So, at  $t=2.00$  sec, the load is given on generator and the system attains the stable condition at  $t=2.5$  sec. After  $t=2.5$  sec various transient conditions are simulated. At  $t=3.00$  sec, the solar irradiation increases which leads to increase in the output active power of SPV system. The power in the system remains balanced as the power generated is equal to power consumption. The BESS works as supporting part of the system which charges and discharges the battery according to the requirements. So, when there is excess of power, the battery works as storage element and when there is lack of power, it works as power source. At  $t=3.5$  sec, the load on phase A goes OFF. So, the power required by load decreases significantly, but this power is diverted to battery so the stability of the system could be maintained. At  $t=4.00$  sec, the load on phase A is restored again and the battery now delivers power required by compensator. But at  $t=4.2$  sec the wind speed increases; the active power output of wind generator also increases. So, to maintain the power balance the battery again works as an energy storage element. The reactive power is injected in the system by the



capacitor bank. The SEIG draws the reactivepower to work as a generator and produce electrical power. The change in loading condition also affects the required reactive power of generator.

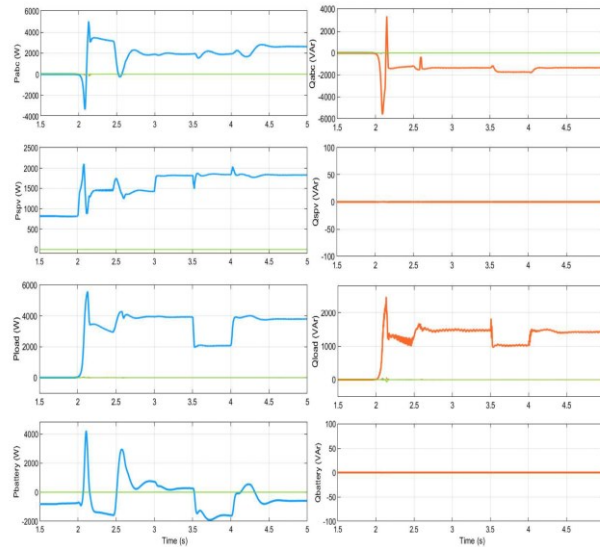


Fig. 9. (a) Pabc = Active power of generator, (b) Pspv = Active power of SPV, (c) Pload = Active power of Load, (d) Pbattery = Active power of Load, (e) Qabc = Reactive power of generator, (f) Qspv = Active power of SPV, (g) Qload = Active power of Load, (h) Qbattery = Active power of Load.

**Case(e):**The operation of the SPV system from  $t=0.50$  sec to  $t=5.00$  sec is shown in fig (10) which includes all the transient duration simulated. The output of solar power is mainly dependent on the irradiation available. After the system achieves stability at  $t=2.5$  sec, the irradiance is increased from  $800 \text{ w/m}^2$  to  $1000 \text{ w/m}^2$  at  $t=3$  sec. Due to this change in irradiance the output power of SPV system also increases. The SPV system is connected across the BESS unit so at  $t=3.5$  sec due to unbalanced loading condition the BESS work as a dump load and hence the voltage across it increases, which in turn increase the voltage across SPV system. At  $t=4$  sec when load is restored, the voltage again comes back to its normal value. The small deviation in the graph of power is due to action of compensator during transient condition.

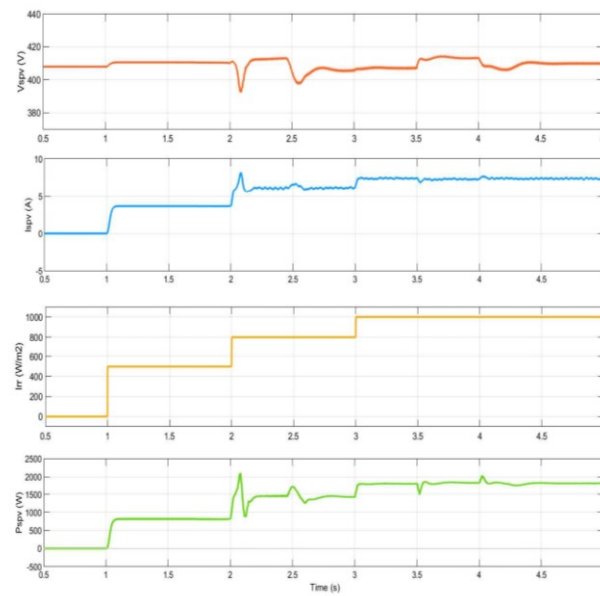


Fig. 7. (a) Vspv = Voltage of SPV, (b) Ispv = current of SPV, (c) Irr = Irradiation of SPV, (d) Pspv = Power of SPV

## 5. CONCLUSION

The proposed system's performance is been simulated in MATLAB/Simulink. The system is designed to extract maximum power from renewable energy sources, while maintaining the system stability irrespective of condition. The system works satisfactorily in various conditions simulated throughout the paper. The SEIG and SPV system is supplying the power to nonlinear/linear loads in proposed system. The DROGI-FLL is used for the control of VSC, and the VSC also works satisfactory and balances the system in dynamic conditions. The voltage and frequency of the system is almost remained constant in all the conditions simulated. The P&O MPPT also works satisfactorily as the SPV system works at MPP. The star double delta transformer used for neutral current compensation also does satisfactory work.

A wind-solar based renewable power generation system operating at isolated location was proposed in this paper. The DROGI-FLL based algorithm was used for the control of the system. The control works sufficiently well and maintained the system stability in various simulated conditions. Other than stability issues, the problems like load balancing, neutral current compensation, reactive power compensation of load were also solved. The P&O MPPT along with boost converter was also used in this paper to maximize the output of SPV system. The complete wind-solar based system was simulated in MATLAB/Simulink.

## 6. APPENDIX

Parameters	Values
Wind generator rating	V = 240 v HP = 5 F = 50 Hz Pole = 4
Wind generator parameters	$L_m = 0.07669$ H $R_s = 0.39390$ $\Omega$ $L_s = 0.00202$ H $R_r' = 0.47910$ $\Omega$ $L_r' = 0.00252$ H
Capacitor for self-excitation	227 $\mu$ F
Compensator parameter	$L_s = 3$ mH $C_{DC} = 8000$ $\mu$ F
BESS parameters	V = 400 v Ah = 7.5 Type = lead-acid SoC = 40%
Load parameters	Phase A and C (with Diode Bridge connected) $R = 7$ $\Omega$ $L = 100$ mH Phase B (Linear load) $R = 7$ $\Omega$ $L = 100$ mH
Wind turbine parameters	Radius of swept area = 1.841m $C_p(\eta, \Theta) = 0.48$ $\beta = 1.12$ $V_\omega = 12$ m/s
Star/Double delta transformer	kVA = 6.5
Boost converter	$C_{in} = 1000$ $\mu$ F $C_{out} = 3000$ $\mu$ F $L_{in} = 1$ mH

PV array	Rated power = 2984 watt Open circuit voltage = 254.1v Short circuit current = 15.68 A Voltage at maximum power = 203v Current at maximum power = 14.7A Total number of strings in series = 7 Total number of strings in parallel = 2
----------	--

**Data Availability.** Data underlying the results presented in this paper are available from the corresponding author upon reasonable request.

**Funding.** There is no funding for this work.

**Conflicts of interest.** The authors declare no conflict of interest.

**Ethics.** The authors declare that the present research work has fulfilled all relevant ethical guidelines required by COPE.



This article is licensed under a Creative Commons Attribution 4.0 International License.

©The Author(s) 2024

## REFERENCES

- [1] Roy, A., & Bandyopadhyay, S. (2019). **“Wind Power Based Isolated Energy Systems”**. Cham: Springer International Publishing.
- [2] Salameh, Z. (2014). **“Renewable energy system design”**. Academic press.
- [3] Borbely, A. M., & Kreider, J. F. (Eds.). (2001). **“Distributed generation: the power paradigm for the new millennium”**. CRC press.
- [4] Stiebler, M. (2008). **“Wind energy systems for electric power generation”**. Springer Science & Business Media.
- [5] Simoes, M. G., & Farret, F. A. (2007). **“Alternative energy systems: design and analysis with induction generators”** (Vol. 13). CRC press.
- [6] Rathore, U. C., & Singh, S. (2014, December). **“Power quality control of SEIG based isolated pico hydro power plant feeding non-linear load”**. In *2014 IEEE 6th India International Conference on Power Electronics (IICPE)* (pp. 1-5). IEEE.
- [7] Bonert, R., & Rajakaruna, S. (1998). **“Self-excited induction generator with excellent voltage and frequency control”**. *IEE Proceedings-Generation, Transmission and Distribution*, 145(1), 33-39.
- [8] Singh, B., Murthy, S. S., & Gupta, S. (2006). **“Analysis and design of electronic load controller for self-excited induction generators”**. *IEEE transactions on energy conversion*, 21(1), 285-293.
- [9] Singh, B., Murthy, S. S., & Gupta, S. (2003, November). **“An improved electronic load controller for self-excited induction generator in micro-hydel applications”**. In *IECON'03. 29th Annual Conference of the IEEE Industrial Electronics Society (IEEE Cat. No. 03CH37468)* (Vol. 3, pp. 2741-2746). IEEE.
- [10] Timorabadi, H. S. (2006, May). **“Voltage source inverter for voltage and frequency control of a stand-alone self-excited induction generator”**. In *2006 Canadian Conference on Electrical and Computer Engineering* (pp. 2241-2244). IEEE.
- [11] Guo, H., Crossley, P., & Terzija, V. (2013, June). **“Impact of battery energy storage system on dynamic properties of isolated power systems”**. In *2013 IEEE Grenoble Conference* (pp. 1-6). IEEE.
- [12] Narayanan, V., Kewat, S., & Singh, B. (2020). **“Solar PV-BES based microgrid system with multifunctional VSC”**. *IEEE Transactions on Industry Applications*, 56(3), 2957-2967.
- [13] Andea, P., Mnerie, A. V., Solomonesc, F., Pop, O., & Cristian, D. (2010, May). **“Conventional vs. alternative energy sources overview. Part II. European strategies”**. In *2010 International Joint Conference on Computational Cybernetics and Technical Informatics* (pp. 601-606). IEEE.
- [14] Ibrahim, O., Yahaya, N. Z., Saad, N., & Umar, M. W. (2015, October). **“Matlab/Simulink model of solar PV array with perturb and observe MPPT for maximising PV array efficiency”**. In *2015 IEEE conference on energy conversion (CENCON)* (pp. 254-258). IEEE.
- [15] Kanjiya, P., Khadkikar, V., & El Moursi, M. S. (2015). **“A novel type-1 frequency-locked loop for fast detection of frequency and phase with improved stability margins”**. *IEEE Transactions on Power Electronics*, 31(3), 2550-2561.

- [16] Busada, C. A., Jorge, S. G., Leon, A. E., & Solsona, J. A. (2011). “**Current controller based on reduced order generalized integrators for distributed generation systems**”. *IEEE Transactions on Industrial Electronics*, 59(7), 2898-2909.
- [17] Eram, T., & Chapman, P. L. (2007). “**Comparison of photovoltaic array maximum power point tracking techniques**”. *IEEE Transactions on energy conversion*, 22(2), 439-449.
- [18] Giri, A. K., Arya, S. R., & Maurya, R. (2018). “**Compensation of power quality problems in wind-based renewable energy system for small consumer as isolated loads**”. *IEEE Transactions on Industrial Electronics*, 66(11), 9023-9031.